Ad Hoc Networks 103 (2020) 102164

Contents lists available at ScienceDirect

Ad Hoc Networks

journal homepage: www.elsevier.com/locate/adhoc

Analysis of compressive sensing and energy harvesting for wireless multimedia sensor networks

Nazli Tekin*, Vehbi Cagri Gungor

Abdullah Gul University, Department of Computer Engineering, Kayseri 38080, Turkey

ARTICLE INFO

Article history:
Received 18 October 2019
Revised 26 January 2020
Accepted 29 March 2020
Available online 3 April 2020

Keywords:
Compressive sensing
Energy harvesting
Network lifetime
Industrial wireless sensor networks

ABSTRACT

One of the main concerns of Wireless Multimedia Sensor Networks (WMSNs) is the huge data size causing the higher energy consumption in transmission. The high energy consumption is a critical problem for lifetime of network includes sensor nodes with limited battery. The data size reduction and Energy Harvesting (EH) methods are the promising solutions to improve the network lifetime. The main objective of this paper is to evaluate the impact of the different data size reduction methods, such as image compression and Compressive s Sensing (CS), and EH methods, such as vibration, thermal and indoor solar, on WMSNs lifetime in industrial environments. In addition, a novel Mixed Integer Programming (MIP) framework is proposed to maximize the network lifetime when EH, CS, and Error Control (EC) approaches are utilized together. Comparative performance results show that utilizing Binary Compressive Sensing (BCS) and Indoor Solar Harvester (ISH) extends industrial network lifetime significantly.

© 2020 Elsevier B.V. All rights reserved.

1. Introduction

Recently, Wireless Multimedia Sensor Networks (WMSNs) have become popular for industrial applications due to their varius application areas and low cost. The main applications of WMSNs include industrial automation systems, condition monitoring systems and environment control systems [1]. In industry, factories can be utilized from WMSNs for monitoring applications. For instance, any failures in manufacturing process, causing high repair cost, can be prevented by WMSN-based early warning systems [2]. In addition to failure detection, the performance and utilization of industrial machines and devices can be monitored and controlled using WMSNs to improve the system efficiency. Furthermore, environment monitoring applications utilizing industrial mobile robots with multimedia sensors take advantage of WMSNs to maintain the quality of service [3].

Due to battery powered sensor nodes with limited energy supply, WMSNs suffer from the large volume of data transmissions. This is because the large volume of data induces higher level of energy consumption in wireless communication. To deal with large amount of data with limited energy sources, some compression algorithms have been developed recently [4–6]. Eliminating redundancy data on image by compression considerably reduces the energy consumption in transmission process. However, the extra energy consumption for computation process emerges. Therefore, there is a trade-off between computation and transmission process in terms of energy consumption in WMSNs.

Additionally, Compressive Sensing (CS) approach for sparse signals has been introduced [7] as a promising solution to compress large amount of data. CS efficiently acquires the data with fewer number of samples than Nyquist theory [8]. In WMSNs, sensor nodes using CS acquire a raw image data which is sparse in transform domain with fewer number of measurements to relay the sink node. The sink node reconstructs the image, where the quality of reconstruction depends on sparsity level of signals.

In industrial WSNs, energy harvesting (EH) methods help to prolong network lifetime by utilizing ambient energy. Energy harvesters can convert ambient energy into electrical energy [9]. The potential sources of energy harvesters for industrial environments are indoor solar, vibration and thermal energy [10]. The main objective of this paper is to evaluate the impact of the different data size reduction methods, such as image compression and CS, and EH methods, such as vibration, thermal and indoor solar, on WMSN lifetime in industrial environments. To this end, the main contributions of our study are summarized as follows:

- The impacts of utilizing CS, image compression and EH methods on network lifetime is examined. For a realistic assessment, the performance evaluations have been conducted by considering acquisition, computation and communication energy dissipation of real-world WMSNs.

* Corresponding author.
E-mail addresses: nazli.tekin@agu.edu.tr (N. Tekin), cagri.gungor@agu.edu.tr (V.C. Gungor).

https://doi.org/10.1016/j.adhoc.2020.102164
1570-8705/© 2020 Elsevier B.V. All rights reserved.

Table 1
Literature overview.

Existing studies	Channel model	Error control	Compressive sensing	Application reliability	Energy harvesting
[11]	✗	✗	✗	✗	✗
[12]	✗	✗	✗	✗	✗
[13]	✗	✗	√	√	✗
[14]	✗	✗	√	✗	✗
[15]	✗	✗	√	✗	✗
[16]	✗	✗	√	✗	✗
[17]	✗	✗	√	✗	✗
Proposed system	√	√	√	√	√

- The proposed analysis considers both realistic channel model for industrial environments and reliability of the network. To identify industrial channel characteristics, the log normal shadowing model is applied.
- To balance the trade-offs between network reliability and lifetime, the node level application of EC scheme approaches is employed.
- A novel Mixed Integer Programming (MIP) framework is formulated to maximize network lifetime, when EH, CS, and image compression are utilized.

The rest of paper is organized as follows. Section 2 provides the previous work in literature. Section 3 presents the system models. Section 4 discusses the performance evaluations and results. Section 5 gives the conclusion.

2. Related work

WMSNs have limited resources with regard to battery and bandwidth constraints. Therefore, energy efficient approaches are essential for WMSNs applications. For multimedia communications, there are some studies based on image compression and CS to reduce the energy consumption. For instance, Lecuire et. al [11] proposed the energy efficient Discrete Cosine Transform (DCT) based image compression scheme. They applied 8×8 DCT coefficients to transform data which leads to less number of operations. They achieved the energy efficient image compression algorithm by saving energy owing to process a few number of DCT coefficients. Sun et. al [12] proposed Low Energy Image Compression Algorithm (LEICA) for WMSNs. The algorithm compresses the image data with high ratio while maintaining the quality of the interest area on image. They showed that LEICA can prolong the network lifetime by reducing energy consumption of both computation and transmission. Wang et. al [13] proposed energy efficient image compressive transmission scheme. They introduced background subtraction of image and block CS to reduce the energy consumption. The performance results show that the proposed scheme contributes to the energy efficient image transmission. Zang et. al [14] proposed an adaptive block CS for wireless image sensor networks. The sampling rate for an each image block is adaptively arranged according to the standard deviation of the block. For instance, the image block with much information has more sampling rate for true reconstruction. As a result, they showed that the proposed algorithm improves the reconstructed image quality effectively. Nandihini et. al [15] implemented the CS for image transmitting. They proposed sensing scheme based on Toeplitz matrix. The results show that proposed sensing matrix has better PSNR values compared to the conventional matrix. Cao et. al [16] proposed data collection algorithm by using CS. They analyzed the energy consumption of sensor node and network lifetime while using the proposed algorithm. They show that the CS based collection algorithm improve network lifetime greatly. Hemalatha et. al [17] proposed energy efficient CS based image transmission algorithm. The proposed CS based image transmission method is considerably better than the conventional methods in terms of energy consumption. The review of previous studies on energy efficient image transmission is presented at Table 1. Some studies proposed new approaches to reduce energy consumption in image transmission by utilizing CS [13–16] or image compression [11,12]. Hemalatha et al. [17] investigated and compared the CS with the other conventional methods. However, none of them focuses on analyzing and comparing the effects of CS and image compression on network lifetime while considering network reliability and EH. In this study, our objective is to investigate the impact of the CS, image compression as well as EH methods, such as vibration, thermal and indoor solar, on WMSN lifetime while considering both channel characteristics and network reliability. To balance the trade-off between network reliability and lifetime, we also evaluate the effects of different EC schemes, such as ARQ, FEC, HARQ on WMSN network lifetime. In addition, a novel Mixed Integer Programming (MIP) framework is proposed to maximize the network lifetime, when EH, CS, and error control approaches are utilized together.

3. System model

In this section, we present the methods considered in our performance evaluations. In No Processing (NP) method, N byte image data is transmitted without any processing. Therefore, only transmission time and transmission energy are considered for network lifetime analysis. In Transform Coding (TC) method, the N byte captured image data is divided into 8×8 image blocks. These image blocks are transformed into frequency domain by using DCT. Later, the K largest values are quantified to achieve K-sparse signal and transmitted to the receiver side. The transmitted K values are decoded at the receiver side and placed their locations. Inverse DCT (IDCT) is applied to the received data for the image reconstruction. In CS method, the captured image is divided into 8×8 image blocks and sparsified by utilizing DCT. M compressed measurements are acquired and transmitted according to sparsity level of the signal. The receiver decodes the K-sparse signals to reconstruct the image. In the BCS method presented by Hemelatha et. al [17], the image is divided into 8×8 blocks and sparsified using Binary DCT (BinDCT). BinDCT only uses addition and shift operations in computation which leads to the significant energy reduction. For TC, CS and BCS, in addition to the transmission and receiving energy, processing data energy should be also considered for network lifetime analysis.

3.1. Compressive sensing

For proper reconstruction in conventional signal processing, a signal is acquired according to the Nyquist theory. The acquired signal is represented as an one dimensional vector $x \in R^N$ [18]. Any vector in R^N can be depicted as a linear combination of basis vec-

tors $\{\psi_i\}_i^N$ as

$$x = \sum_{i=1}^{N} s_i \psi_i \qquad x = \Psi s, \tag{1}$$

where ψ is the basis matrix with ith column ψ_i. N is the number of measurement required for full signal acquisition. A signal is K-sparse when the K of coefficients are non-zero. In compression method based on transform coding, N measurements are acquired. Considering the all transform coefficients, only the largest K coefficients are encoded and transmitted where $K < N$ to reduce the transmitted data. However, in CS M random measurements which $M < < N$ is acquired and transmitted. The number of M measurement determined according to sparsity of signal where $M \geq \alpha K \log(N/K)$ for true reconstruction.

The signal recovery is done by solving the minimum l_1-norm optimization problem shown below

$$\min \|s\|_{l_1} \quad s.t. \quad y = \Phi \Psi s. \tag{2}$$

3.2. Physical layer model

To ensure the reliable communication in industrial environment is critical owing to the interference and noises generated from machines. Thus, we should consider the realistic channel model for better analysis. The path loss, $PL_{ij}(d)$, over link-(i,j) for log normal shadowing model [19] is given by

$$PL_{ij}(d) = PL(d_0) + 10n \log_{10}\left(\frac{d_{ij}}{d_0}\right) + X_\sigma, \tag{3}$$

where d_{ij} is the distance between link-(i,j). d_0 is the reference distance therefore, $PL(d_0)$ is the path loss at reference distance. n, X_σ and σ are the path loss exponent, a Gaussian random variable (in dB) and standard deviation, respectively. Signal-to-noise ratio (γ_{ij}) is estimated as:

$$\gamma_{ij} = P_t - PL_{ij}(d_{ij}) - P_n, \tag{4}$$

where P_t is the output power and P_n is the noise floor. The Bit Error Rate (BER) is computed as [20]

$$P_{b,ij} = \frac{1}{2}\exp^{-\frac{E_b/N_0}{2}}, \tag{5}$$

where

$$E_b/N_0 = \gamma \frac{B_N}{R}, \tag{6}$$

where γ, B_N and R are the received SNR, noise bandwidth, data rate, respectively. Different formulas are applied to calculate the Packet Error Rate (PER) for different EC schemes (*i.e.,* ARQ, FEC). For ARQ, the successful packet transmission probability, p_{ij}^s, is computed as

$$p_{ij}^s(q) = \left(1 - \frac{1}{2}\exp^{-\frac{\gamma_{ij}}{2}\frac{1}{0.64}}\right)^{8q}, \tag{7}$$

where q denotes the packet size in bytes. Thus, PER is shown by

$$PER_{ij}^{ARQ}(q) = 1 - p_{ij}^s(q). \tag{8}$$

For FEC schemes (*e.g.,* BCH and RS), the Block Error Rate, BLER(n,k,t), is shown by [21]

$$BLER_{ij}(n,k,t) = \sum_{l=t+1}^{n}\left(\frac{n}{l}\right)\left(P_{b,ij}\right)^l\left(1 - P_{b,ij}\right)^{n-l}, \tag{9}$$

where n, k and t indicate the block length, payload length and error correcting capability, respectively. The PER is given by

$$PER_{ij}^{FEC}(q,n,k,t) = 1 - \left(1 - BLER_{ij}(n,k,t)\right)^{\lceil \frac{q}{k} \rceil}, \tag{10}$$

where $\lceil \frac{q}{k} \rceil$ is the number of blocks required to send q bits.

3.3. Link layer model

Automatic Repeat Request (ARQ), Forward Error Correction (FEC) and Hybrid ARQ (HARQ) are three type of EC schemes utilized by WSNs. In ARQ schemes, transmitter is informed by receiver sending an acknowledgement packet if loss or erroneous packets occur. Retransmissions are asked from transmitter to recover data packets. The retransmissions lead to extra energy consumption in communication. FEC schemes add the redundant bits to data packet, thus error correction is done by decoding the data packets. The redundant bits and decoding process cause overhead energy consumption for sensor nodes. In this study, we analyse Bose Chaudhuri Hocquenghem (BCH) (*i.e.,* BCH(31,21,5) and BCH(31,11,5)) and Reed Solomon (RS) (*i.e.,* RS(15,11,2). HARQ utilizes both ARQ and FEC scheme codes. HARQ-I and HARQ-II are used for this study. In HARQ-I, data packet with FEC code is retransmitted. In HARQ-II, retransmission occurs only by sending redundant bits.

3.3.1. Communication energy calculations

Communication energy involves the energy consumption during a packet transmission and receiving. For ARQ, the energy consumed by transmitter is derived by

$$E_{tx,ij}^{ARQ} = E_{enc} + n_{ret,ij}^{ARQ}\{(E_{tx}(L_P) + E_{rx}(L_A)) + E_{to}\}. \tag{11}$$

The energy consumed by receiver is determined by

$$E_{rx}^{ARQ} = n_{ret,ij}^{ARQ} \times (E_{rx}(L_P) + E_{tx}(L_A)), \tag{12}$$

where $E_{tx}(x)$ is the transmission energy consumption and $E_{rx}(x)$ is the receiving energy consumption derived in Equation (19). L_P and L_A indicate the payload size and acknowledgement size, respectively. E_{to} is the timeout energy which is calculated as:

$$E_{to} = P_{std} \times \left(T_{pd,ij} + T_{grd}\right) \tag{13}$$

where P_{std} is the standby power. T_{pd} is the propagation time and T_{grd} is the guard time. The probability of successful handshake communication which is transmitting data and receiving acknowledgement is expressed as [30]:

$$p_{ij}^{HS,s} = p_{ij}^s(L_P) \times p_{ji}^s(L_A). \tag{14}$$

The number of retransmission is derived as:

$$n_{ret,ij}^{ARQ} = \frac{1}{p_{ij}^{HS,s}}. \tag{15}$$

The number of retransmission of other error control schemes is taken as 1 (*i.e.,* $n^k{}_{ret,ij}$=1 $k \in$ {FEC, HARQ}). The packet success rate after the retransmission is calculated as [22]:

$$\phi_{ij}^{ARQ} = 1 - \left[1 - p_{ij}^{HS,s}\right]^{(n_{ret,ij}+1)}. \tag{16}$$

For FEC, the energy consumption consumed by transmitter is described by

$$E_{tx,ij}^{FEC} = E_{enc} + E_{tx}(L_P). \tag{17}$$

The receiver consumes extra decoding energy in FEC schemes. Therefore, the energy consumed by receiver is calculated as follows:

$$E_{rx,ij}^{FEC} = (E_{rx}(L_P) + E_{dec}(L_P)). \tag{18}$$

$E_{tx}(x)$ and $E_{rx}(x)$, energy consumed for transmitting and receiving x bits data, are calculated as

$$\begin{aligned} E_{tx}(x) &= E_{elec} \times x + P_{tx}\left(\frac{x}{R}\right) \\ E_{rx}(x) &= E_{elec} \times x + P_{rx}\left(\frac{x}{R}\right), \end{aligned} \tag{19}$$

where P_{tx} and P_{rx} are transmision and receiving power, respectively. R denotes the data rate and E_{elec} denotes to energy consumed by transmitter electronics. $E_{dec}(L_P)$ determines the decoding energy given by

$$E_{dec}(L_P) = P_{proc} T_{dec}(L_P), \tag{20}$$

where P_{proc} is processing power and T_{dec} is time spent during decoding and presented in section (3.3.2). E_{enc} is the encoding energy and negligible [20]. The packet succes rate is given by

$$\phi_{ij}^{FEC} = 1 - PER_{ij}^{FEC}. \tag{21}$$

For HARQ, the energy consumed by transmitter is computed as:

$$E_{tx,ij}^{HARQ} = E_{enc} + E_{tx}(L_{P_f}) + (1 - p_{ij}^{s}(L_{P_f}))(E_{rx}(L_{P_n}) + E_{tx}(L_{P_s})), \tag{22}$$

where L_{P_f}, L_{P_s} and L_{P_n} are the length of first and second transmitted packet and the NACK packet, respectively. $p_{ij}^{s}(L_{P_f})$ refers the probability that the first packet successfully transmitted to the receiver. The receiving energy consumption is shown by

$$E_{rx,ij}^{HARQ} = E_{rx}(L_{P_f}) + E_{dec}(L_{P_f}) + (1 - p_{ij}^{s}(L_{P_f})) (E_{tx}(L_{P_n}) + E_{rx}(L_{P_s}) + E_{dec}(L_{P_s})). \tag{23}$$

The packet success rate is given by

$$\phi_{ij}^{HARQ} = 1 - (PER_{ij}^{ARQ} \times PER_{ij}^{FEC}). \tag{24}$$

3.3.2. Latency analysis

For ARQ, the time spent during transmission and waiting acknowledgement is determined by

$$T_{tx,ij}^{ARQ} = \frac{L_P}{R} + T_{pd,ij} + T_{grd}. \tag{25}$$

The time spent during receiving is shown by

$$T_{rx,ij}^{ARQ} = \frac{L_P}{R}. \tag{26}$$

For FEC, time spent during transmission is shown by

$$T_{tx,ij}^{FEC} = \frac{L_P}{R} + T_{pd,ij}. \tag{27}$$

The time spent during receiving and decoding is shown by

$$T_{rx,ij}^{FEC} = \frac{L_P}{R} + T_{dec}. \tag{28}$$

$T_{dec,bc}$ indicates decoding time for FEC block and is calculated as:

$$T_{dec,bc} = (2nt + 2t^2) \times (T_{add} + T_{mult}), \tag{29}$$

where T_{add} and T_{mult} stand for addition and multiplication time. Mica2 with 8-bit micro-controller operates addition and multiplication of 8 bits in 3 cycles where $m = \lfloor log2n + 1 \rfloor$ [23]. Therefore

$$T_{add} + T_{mult} = 3\frac{m}{t} t_{cycle}, \tag{30}$$

where t_{cycle} is one cycle period and t is taken as 8 due to 8 bit micro-controller. Finally, decoding time is given by

$$T_{dec}(L_P) = T_{dec,bc} \left\lceil \frac{L_P}{k} \right\rceil, \tag{31}$$

where $\lceil \frac{L_P}{k} \rceil$ is the number of block required to send L_P bits. For HARQ, the transmission time is shown by

$$T_{tx,ij}^{HARQ} = T_{tx,ij}^{ARQ} + T_{tx,ij}^{FEC}. \tag{32}$$

For HARQ, the receiving time is shown by

$$T_{rx,ij}^{HARQ} = T_{rx,ij}^{ARQ} + T_{rx,ij}^{FEC}. \tag{33}$$

Table 2
Simulation parameters for energy harvesters.

Indoor solar harvester			
	Description	Value	Unit
T_C	Ambient temperature	295	K
n	Number of PV cells	15	-
I_0	Reverse saturation current	$1 \times 10^{-}9$	A
I_{SC}	Short circuit current	150	μA
q	Electron charge	$1.6022 \times 10^{-}19$	C
k	Boltzman's constant	$1.3807 \times 10^{-}23$	$JK^{-}1$
Thermal harvester			
	Description	Value	Unit
ΔT	Temperature differences	10	K
n	Number of thermocouples	5200	-
α	Seebeck's coefficients	0.21	mV/K
R_s	Electrical resistance	82	$k\Omega$
Vibration harvester			
	Description	Value	Unit
ω	Frequency	71	Hz
V	Voltage	48	V
I	Current	0.05	mA

3.3.3. Computation energy calculations

For both compression (*i.e., TC*) and CS (*i.e., CS and BCS*) methods, the additional energy is spent for processing the data. In TC method, DCT implementation and sorting image block, maximum element and its location selection, and encoding lead to extra computational energy consumption. In CS and BCS methods, the DCT and BinDCT implementation and $M \times N$ Gaussian matrix multiplication, and encoding cause extra computational energy. The computation energy is calculated by multiplying execution time spent for processing data with processing power which is shown by

$$E_{cmp} = P_{proc} \times T_{cmp}, \tag{34}$$

where P_{proc} is processing power and T_{cmp} is execution time for processing data. The processing power (P_{proc}) of Mica2 with Atmel Atmega 128 Processor is given in Table 4. The execution times (T_{cmp}) are presented in Table 5.

3.4. Energy harvesting model

In this study, we use indoor solar, thermal and vibration harvesters for industrial environment The simulation parameters utilized by energy harvesters are shown in Table 2 [24].

3.4.1. Indoor solar harvester

In ISH, photovoltaic cells generate the electrical energy by utilizing artificial light for industrial environments [2]. The current is calculated as

$$I_{PV} = I_L - I_0 \left[\exp\left(\frac{V_{PV} + I_{PV} R_s}{n_s V_t} \right) - 1 \right]. \tag{35}$$

In (35), I_L and I_0 depict the short circuit current (A) and reverse saturation current of the p-n diodes, respectively. R_s denotes the series resistance of the cells (Ω). The thermal voltage, V_t, is given by

$$V_t = \frac{kT_c}{q}, \tag{36}$$

where k, T_c and q are the Boltzmann's constant, cell temperature (K), and electron charge, respectively. The harvested power is expressed as

$$P = V_{PV} I_L - V_{PV} I_0 \left[\exp\left(\frac{V_{PV}}{n_s k T_c / q} \right) \right]. \tag{37}$$

3.4.2. Thermal harvester

The Thermal Harvester (TH) generates electricity from temperature difference by using Seebeck effects [25]. The open-circuit voltage (V_{oc}) is calculated as

$$V_{oc} = S * \Delta T = n * \alpha (T_H - T_C), \tag{38}$$

where S and α indicate the Seebeck's coefficient of TEG and thermocouples, respectively. n is the number of thermocouples in TEG. T_H and T_C are the high and low temperature, respectively. The current is calculated as:

$$I_{TEG} = \frac{V_{oc} - V_{TEG}}{R_{s,TEG}}, \tag{39}$$

where $R_{s,TEG}$ is the internal resistance of TEG. The harvested power is given by

$$P_{TEG} = V_{TEG} I_{TEG} = \frac{V_{TEG} n\alpha (T_H - T_C) - V_{TEG}^2}{R_{s,TEG}}. \tag{40}$$

3.4.3. Vibration harvester

The mechanical energy is converted into electrical power by using piezoelectricity [2]. The harvested power is given by

$$| P | = \frac{m\zeta_e A^2}{4\omega\zeta_T^2}, \tag{41}$$

where m refers to the proof mass, ω refers to the input frequency and A denotes the amplitude of acceleration. ζ_e is the electrical damping ratio and ζ_T is the combined electrical and mechanical damping ratio (*i.e.*, $\zeta_T = \zeta_e + \zeta_m$).

3.5. MIP For maximizing network lifetime

The objective of the framework presented in Fig. 1 is to maximize network lifetime by balancing the energy dissipation of all sensor nodes. The directed graph $G = (V, A)$ symbolizes the network topology. V indicates the set of all sensor nodes whereas W indicates set of all sensor nodes except sink node (*i.e.*, $W = V \backslash \{1\}$). A presents the link between node pairs. Finally, E represents the set of EC schemes (*i.e.*, ARQ, BCH(31,11,5), BCH(31,21,5), RS(15,11,2), HARQ-I and HARQ-II).

The network lifetime is defined as the time passed until the first node drains out its battery. The network lifetime is organized with rounds where T_{rnd} denotes the predefined constant time duration for a round. H denotes the number of round during lifetime. Therefore, $H \times T_{rnd}$ presents the network lifetime. In each round, s_i number of data packets are generated by sensor nodes to relay them to the sink node. Node level approach on EC schemes selection is applied in data transmission. In this context, each node decides the utilizing EC schemes according to framework constraints for each transmission. In other words, different node implements the different EC schemes in each transmission such that the choice of EC schemes depends on the requirement of each link to ensure the reliability and energy efficiency.

f_{ij}^k is the decision variable that refers to packet flows over link-(i,j) with k type EC schemes. Equation (42) specifies that no flow over link-(i,j) with all kind of EC schemes (i.e $f_{ij}^k \ \forall (i,j) \in A$) can be negative. Equation (43) guarantees that sink node does not generate data packets. Equation (44) provide the flow balance such that the number of incoming packets plus generated packets are equal to the number of outgoing packets for each sensor nodes. ϕ_{ij}^k denotes the packet success rate. Equation (45) ensures that sink node receives at least r percent of data packets generated by all sensor nodes. r is the desired reliability rate and takes value from 0.5 to 0.9. In equation (46), $T_{busy,i}$ is the total time that a node spends for acquiring, transmitting and receiving. $n_{ret,ij}^k$ is the number of retransmission. Equation (47) ensures that total amount of energy consuming for acquisition, communication and computation can not exceed the batery capacity of a sensor node. P_{harv} which is the average harvested power given in Table 3 supplies additional energy sources besides the battery. Equation (48) indicates that the bandwidth needed for transmitting and receiving must be smaller than the channel bandwidth.

Table 3
Average harvested power.

Harvester	Value	Unit
Indoor solar	0.4947	mW
Thermal	0.3635	mW
Vibration	0.2400	mW

Table 4
Simulation parameters.

Channel characteristics		
	Description	Value
PL(d_0)	Path loss at distance, d_0 [26]	63.57 dB
d_0	Reference distance	0.5 m
n	Path loss exponent [26]	2.40
σ	Shadowing standard deviation [26]	4.79 dB
P_n	Noise Floor	-93.0 dBm
P_t	Output power	0 dB
R	Data rate	19.2 kbps
B_N	Noise bandwidth	30 kHz kbps
Hardware characteristics		
	Description	Value
P_{tx}	Transmission power	5 mW
P_{rx}	Receiving power [27]	21 mW
P_{proc}	Processing power [23]	24 mW
P_{slp}	Sleep power [28]	0.3 mW
ξ	Initial battery energy	25 kJ
t_{cycle}	Cycle duration [23]	250 ns
E_{acq}	Acquisition energy [29]	600 µJ
T_{acq}	Acquisition time	20 ms
E_{elec}	Electronics energy	50 nJ
L_P	Payload size	128 byte
L_A	Acknowledgement size	20 byte

Table 5
Compression results and Execution Time of an 8 × 8 image block for different sparsity level.

Method	Compression results (bpp)		
	K = 2	K = 3	K = 4
TC	0.55	0.8	1.03
CS	1.49	2.25	3.17
BCS	0.59	1.44	2.26
Method	Execution Time (ms)		
	K=2	K=3	K=4
TC	80.39	80.58	80.77
CS	79.09	80.85	83.74
BCS	12.50	14.74	17.59

4. Performance analysis

In performance evaluations, sensor nodes are deployed randomly in disk shaped connected network with various network radius (R_{net}). The base station is located at (0,0). Each sensor node in the network generates s number of data packets from N byte image data at each round. The number of data packets is calculated as $s = \lceil \frac{N}{L_P - L_H} \rceil$ where L_P and L_H are packet size and header size, respectively. The generated packets are relayed to the base station. To maximize network lifetime, we build the proposed MIP framework shown in Fig. 1 which takes into account the energy con-

Maximize H
Subject to:

$$f_{ij}^{k} \geq 0, \forall (i,j) \in A, \forall (k) \in E \tag{42}$$

$$f_{1j}^{k} = 0, \forall (j) \in W, \forall (k) \in E \tag{43}$$

$$\sum_{k \in E} \sum_{(i,j) \in A} f_{ij}^{k} - \sum_{k \in E} \sum_{(j,i) \in A} f_{ji}^{k} \times \phi_{ji}^{k} = H \times s_i, \forall i \in W \tag{44}$$

$$\sum_{k \in E} \sum_{(j,1) \in A} f_{j1}^{k} \times \phi_{j,1}^{k} \geq \sum_{i \in W} s_i \times H \times r, \forall i \in W \tag{45}$$

$$\begin{aligned} T_{busy,i} = & \sum_{k \in E} \sum_{i \in W} T_{tx,ij}^{k} \times f_{ij}^{k} \times n_{ret,ij}^{k} \\ & + \sum_{i \in W} T_{rx,ji}^{k} \times f_{ji}^{k} \times n_{ret,ji}^{k} \\ & + H \times (T_{acq} + T_{cmp}), \forall i \in W \end{aligned} \tag{46}$$

$$\begin{aligned} & \sum_{k \in E} \sum_{j \in W} E_{tx,ij}^{k} \times f_{ij}^{k} + \sum_{k \in E} \sum_{j \in W} E_{rx,ji}^{k} \times f_{ji}^{k} \\ & + H \times (E_{acq} + E_{cmp}) + P_{slp} \times (H \times T_{rnd} - T_{busy,i}) \\ & - P_{harv} \times T_{harv} \times H \leq \xi, \forall i \in W \end{aligned} \tag{47}$$

$$\begin{aligned} (L_P + L_A) \times \sum_{k \in E} \sum_{j \in W} f_{ij}^{k} \times n_{ret,ij}^{k} + \sum_{k \in E} \sum_{j \in W} f_{ji}^{k} \times n_{ret,ji}^{k} \\ \leq \varsigma \times H \times T_{rnd} \forall i \in V \end{aligned} \tag{48}$$

Fig. 1. The MIP framework that maximizes network lifetime.

sumption of both computational and communication energy dissipation. In each round where T_{rnd} taken as an hour for this evaluations, sensors acquire an image data to transmit to the sink node. In addition, it is assumed that the sensors harvest energy for 10 minutes in each round. For solving our MIP model, we utilize General Algebraic Modelling System (GAMS) and MATLAB. We present the average values obtained from 100 different simulation results in figures. Simulation parameters are shown in Table 4.

As performance metrics, we define the application reliability rate as the ratio between the number of received data packets by sink node and the number of data packets generated by all sensors in the network. We also define the lifetime improvement as the percentage of network lifetime increase when an EH, image compression or CS are utilized separately or jointly.

In Fig. 2a–c, lifetime improvement refers to percent of lifetime gain of TC, CS and BCS with respect to NP. Fig. 2a presents the impact of all data size reduction methods used in image transmission as a function of network radius (R_{net}). For all values of R_{net}, image transmission using BCS gives the best network lifetime improvement owing to BCS's least computational energy versus the other methods. Until the R_{net} reaches 12 m, the lifetime with image transmission using NP is larger than that of TC and CS. The reason for that mostly one hop transmissions prevent the energy consumption of relay nodes occur in smaller network. As a result, the lifetime improvement for TC and CS at 10 m takes negative values. The network lifetime using TC in image transmission is larger than that of the CS. Although the computational energy values of both methods are closed, the compression ratio of TC is greater than CS, which leads to less data transmission and thus less energy consumption in transmission.

Fig. 2 b presents the lifetime improvement as a function of reliability rate. The absolute value of network lifetime diminishes, while reliability rate increases. Since the constant transmission over the same node while trying to ensure desired reliability rate leads to faster battery depletion of that node. However, as the reliability rate increases, the lifetime improvement also increases. This shows that when the desired application reliability is high, the data reduction methods (*i.e.,* TC, CS, BCS) provides higher development with regard to image transmission with NP. Fig. 2c presents the lifetime improvement with various sparsity level. The compression ratio and execution time for an image block varying according to sparsity level are shown in Table 5 [17]. As the sparsity level increases, the lifetime improvement decreases. In addition, increase in bits per pixel (bpp) means decrease in data size reduction. Higher data size and execution time lead to higher energy consumption in transmission and computation, respectively.

In Fig. 3a, b and –c, lifetime improvement refers to the percent of EH contributions on industrial network lifetime. Fig. 3a illustrates the effect of EH methods on network lifetime using NP in image transmission with respect to the changing R_{net}. As the network area gets larger, the lifetime improvement decreases for all type of EH methods (*i.e.,* vibration,thermal and indoor solar).

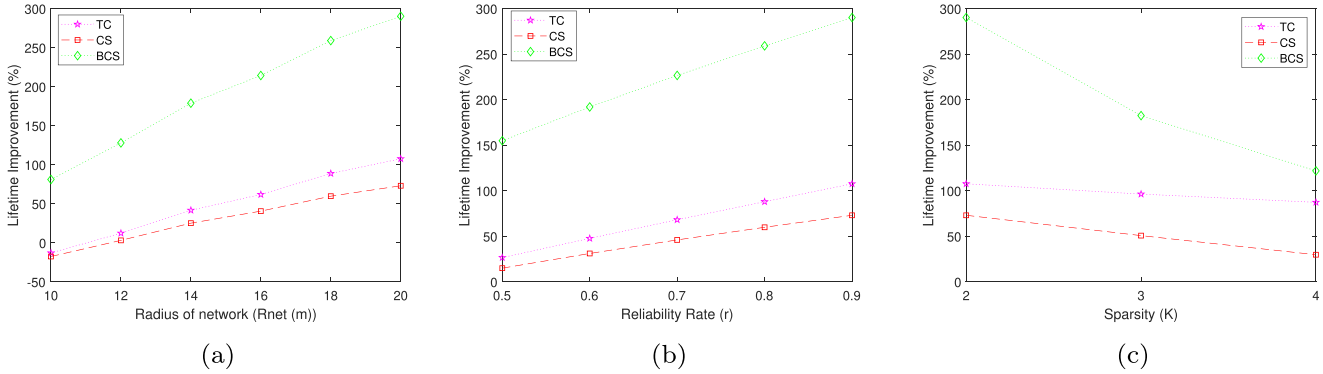

Fig. 2. Lifetime Improvement as a function of (a) network radius (R_{net}) where r=0.9 and K=2 (b) reliability rate (r) where R_{net}=20m and K=2 (c) sparsity level (K) where R_{net}=20m and r=0.9.

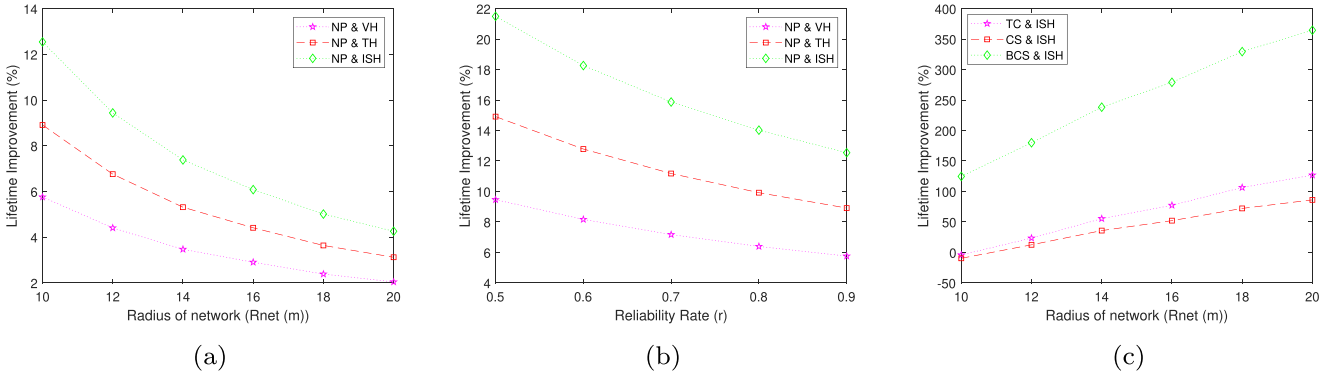

Fig. 3. Lifetime Improvement as a function of network radius (R_{net}) for (a) various harvesters (b) various image transmission approaches with indoor solar harvester (c) various image transmission approaches with indoor solar harvester where r=0.9 and K=2.

ISH provides the most lifetime improvement, which is nearly 13 % when R_{net}=10 m, r=0.9 and K=2. Since ISH performs the greatest lifetime improvement, we continue with the ISH for the rest of evaluations. Fig. 3b depicts the impact of EH methods on network lifetime with regard to changing reliability rate. It is clearly seen that, as the reliability rate increases the lifetime improvement decreases. When the reliability rate is 0.5, the lifetime improvement reaches near 22 %, whereas when reliability rate is 0.9 it decreases to 13 %. Fig. 3c shows the amount of development on network lifetime when using both data size reduction approaches and ISH. CS and TC with ISH prolong the network lifetime 86 % and 126 %, respectively, whereas BCS with ISH prolong network lifetime 364 % according to NP with no EH.

The proposed optimization model that maximizes the network lifetime in industrial environments is an MIP problem, which is known to be an NP-complete problem. The efficient heuristics are required to decrease the computational complexity of MIP problem. To this end, linear programming (LP) relaxation method is applied to solve the proposed optimization problem where integer variable of the original MIP problem are taken as continuous variable. Here it is important to note that the LP problems can be solved in polynomial time. Table 6 presents the average solution time as a function of R_{net}. The average solution time is calculated by averaging 100 trials of each R_{net} value for NP, TC, CS and BCS, when reliability rate (r) and sparsity level (K) are set to 0.9 and 2, respectively. The average solution times are executed on Intel i5 machine with 12GB RAM. Based on performance evaluations, BCS has the lowest average solution time that are between 0.88 and 1.38. The average solution time of CS are between 1.26 and 1.50. The average solution time of TC are between 1.06 and 1.44. Finally, NP has the highest average solution time that is between 1.73 and 2.24.

Table 6
Average Solution Time as a function of R_{net}.

Average Solution Time (s)				
R_{net} (m)	NP	TC	CS	BCS
10	2.24	1.30	1.50	1.33
12	2.05	1.25	1.40	1.38
14	1.95	1.44	1.36	1.35
16	2.04	1.43	1.26	1.30
18	1.79	1.09	1.40	1.31
20	1.73	1.06	1.33	0.88

5. Conclusions

In WMSNs, image transmission requires higher energy than regular data transmission due to huge amount of data. Thus, data size reduction before transmission become very critical for WMSNs. In this paper, we examine the impact of image compression and CS methods on WMSN lifetime. To achieve this, we formulate the Mixed Integer Programming (MIP) framework, which maximizes the network lifetime by considering both communication and computation energy dissipation of real-world WMSNs. To adopt realistic channel model, we utilize log normal shadowing model for industrial networks. We also consider EC approaches and their energy consumption to provide desired application reliability. Additionally, to prolong the network lifetime, we apply convenient EH methods (*i.e.,* vibration, thermal, indoor solar) for industrial environments.

The main conclusions of this paper are listed as follows:

- The performance results show that BCS offers better lifetime than the other data size reduction models due to its lowest

computation energy. For all data reduction models, increasing sparsity level results in high execution time and low compression leading to decrease in network lifetime. In addition, the network lifetime decreases when network reliability rate is increased.

- Among all harvesters, ISH outperforms the other harvesters, such as VH and TH. ISH can provide the lifetime improvement at least 5 % and at most 13 % when the reliability rate is 0.9.
- The utilization of only BCS algorithm extends the lifetime up to 300 %, whereas the joint utilization of BCS and ISH extends the industrial network lifetime up to 364 % compared to network lifetime with NP method.

As a future work, we plan to analyze the effects of node level and network level EC implementations on industrial network lifetime. In addition, the experimental evaluations of proposed approaches via WMSN testbeds is another important future work.

Declaration of Competing Interest

The authors whose names are listed immediately below certify that they have NO affiliations with or involvement in any organization or entity with any financial interest (such as honoraria; educational grants; participation in speakers bureaus; membership, employment, consultancies, stock ownership, or other equity interest; and expert testimony or patent-licensing arrangements), or non-financial interest (such as personal or professional relationships, affiliations, knowledge or beliefs) in the subject matter or materials discussed in this manuscript.

References

[1] M. Bal, Industrial applications of collaborative wireless sensor networks: A survey, in: 2014 IEEE 23rd International Symposium on Industrial Electronics (ISIE), IEEE, 2014, pp. 1463–1468.

[2] N. Tekin, H.E. Erdem, V.C. Gungor, Analyzing lifetime of energy harvesting wireless multimedia sensor nodes in industrial environments, Comput. Stand. Interfaces 58 (2018) 109–117.

[3] V.C. Gungor, G.P. Hancke, et al., Industrial wireless sensor networks: challenges, design principles, and technical approaches, IEEE Trans. Ind. Electron. 56 (10) (2009) 4258–4265.

[4] Q. Lu, W. Luo, J. Wang, B. Chen, Low-complexity and energy efficient image compression scheme for wireless sensor networks, Comput. Netw. 52 (13) (2008) 2594–2603.

[5] L. Makkaoui, V. Lecuire, J.-M. Moureaux, Fast zonal DCT-based image compression for wireless camera sensor networks, in: 2010 2nd International Conference on Image Processing Theory, Tools and Applications, IEEE, 2010, pp. 126–129.

[6] O. Ghorbel, W. Ayedi, M.W. Jmal, M. Abid, Dct & dwt images compression algorithms in wireless sensors networks: comparative study and performance analysis, Int. J. Wirel. Mobile Netw. 4 (6) (2012) 45.

[7] D.L. Donoho, et al., Compressed sensing, IEEE Trans. Inf. Theory 52 (4) (2006) 1289–1306.

[8] S. Li, L. Da Xu, X. Wang, Compressed sensing signal and data acquisition in wireless sensor networks and internet of things, IEEE Trans. Ind. Inf. 9 (4) (2012) 2177–2186.

[9] F.K. Shaikh, S. Zeadally, Energy harvesting in wireless sensor networks: acomprehensive review, Renew. Sustain. Energy Rev. 55 (2016) 1041–1054.

[10] Y.K. Tan, S.K. Panda, Energy harvesting from hybrid indoor ambient light and thermal energy sources for enhanced performance of wireless sensor nodes, IEEE Trans. Ind. Electron. 58 (9) (2010) 4424–4435.

[11] V. Lecuire, L. Makkaoui, J.-M. Moureaux, Fast zonal DCT for energy conservation in wireless image sensor networks, Electron. Lett. 48 (2) (2012) 125–127.

[12] E. Sun, X. Shen, H. Chen, A low energy image compression and transmission in wireless multimedia sensor networks, Procedia Eng. 15 (2011) 3604–3610.

[13] Y. Wang, D. Wang, X. Zhang, J. Chen, Y. Li, Energy-efficient image compressive transmission for wireless camera networks, IEEE Sens. J. 16 (10) (2016) 3875–3886.

[14] J. Zhang, Q. Xiang, Y. Yin, C. Chen, X. Luo, Adaptive compressed sensing for wireless image sensor networks, Multimed. Tools Appl. 76 (3) (2017) 4227–4242.

[15] S.A. Nandhini, S. Radha, P. Nirmala, R. Kishore, Compressive sensing for images using a variant of toeplitz matrix for wireless sensor networks, J. Real-Time Image Process 16 (2019) 1525–1540.

[16] G. Cao, F. Yu, B. Zhang, Improving network lifetime for wireless sensor network using compressive sensing, in: 2011 IEEE International Conference on High Performance Computing and Communications, IEEE, 2011, pp. 448–454.

[17] R. Hemalatha, S. Radha, S. Sudharsan, Energy-efficient image transmission in wireless multimedia sensor networks using block-based compressive sensing, Comput. Electric. Eng. 44 (2015) 67–79.

[18] C. Caione, D. Brunelli, L. Benini, Compressive sensing optimization for signal ensembles in WSNs, IEEE Trans. Ind. Inf. 10 (1) (2013) 382–392.

[19] M. Zuniga, B. Krishnamachari, Analyzing the transitional region in low power wireless links, in: Sensor and Ad Hoc Communications and Networks, 2004. IEEE SECON 2004. 2004 First Annual IEEE Communications Society Conference on, IEEE, 2004, pp. 517–526.

[20] M.C. Vuran, I.F. Akyildiz, Error control in wireless sensor networks: a cross layer analysis, IEEE/ACM Trans. Netw. 17 (4) (2009) 1186–1199.

[21] M.C. Domingo, M.C. Vuran, Cross-layer analysis of error control in underwater wireless sensor networks, Comput. Commun. 35 (17) (2012) 2162–2172.

[22] K. Schwieger, A. Kumar, G.P. Fettweis, On the impact of the physical layer on energy consumption in sensor networks, in: EWSN, 2005, pp. 13–24.

[23] M.C. Vuran, I.F. Akyildiz, Cross-layer analysis of error control in wireless sensor networks, in: Sensor and Ad Hoc Communications and Networks, 2006. SECON'06. 2006 3rd Annual IEEE Communications Society on, vol. 2, IEEE, 2006, pp. 585–594.

[24] N. Tekin, V.C. Gungor, The impact of error control schemes on lifetime of energy harvesting wireless sensor networks in industrial environments, Comput. Stand. Interfaces (2020) 103417.

[25] K. Uchida, S. Takahashi, K. Harii, J. Ieda, W. Koshibae, K. Ando, S. Maekawa, E. Saitoh, Observation of the spin seebeck effect, Nature 455 (7214) (2008) 778.

[26] G. Gao, H. Zhang, L. Li, Performance evaluation of WSNs-based link quality estimation metrics for industrial environments, in: Advanced Technologies in Ad Hoc and Sensor Networks, Springer, 2014, pp. 69–79.

[27] V. Shnayder, M. Hempstead, B.-r. Chen, G.W. Allen, M. Welsh, Simulating the power consumption of large-scale sensor network applications, in: Proceedings of the 2nd International Conference on Embedded Networked Sensor Systems, ACM, 2004, pp. 188–200.

[28] C. Eris, M. Saimler, V.C. Gungor, E. Fadel, I.F. Akyildiz, Lifetime analysis of wireless sensor nodes in different smart grid environments, Wirel. Netw. 20 (7) (2014) 2053–2062.

[29] G. Anastasi, A. Falchi, A. Passarella, M. Conti, E. Gregori, Performance measurements of motes sensor networks, in: Proceedings of the 7th ACM International Symposium on Modeling, Analysis and Simulation of Wireless and Mobile Systems, ACM, 2004, pp. 174–181.

[30] H.U. Yildiz, V.C. Gungor, B. Tavli, A hybrid energy harvesting framework for energy efficiency in wireless sensor networks based smart grid applications, In: 17th Annual Mediterranean Ad Hoc Networking Workshop (Med-Hoc-Net) (2018).

Nazli Tekin received her B.S. degree in computer engineering from Koc University,Istanbul, Turkey, in 2011. She is currently Ph.D. student in electrical and computer engineering at Abdullah Gul University,Turkey. Her current research area is Wireless Sensor Networks.

V. Cagri Gungor received his B.S. and M.S. degrees in electrical and electronics engineering from Middle East Technical University, Ankara, Turkey, in 2001 and 2003, respectively. He received his Ph.D. degree in electrical and computer engineering from the Broadband and Wireless Networking Laboratory, Georgia Institute of Technology, Atlanta, GA, USA, in 2007. Currently, he is an Professor and Chair of Computer Engineering Department, Abdullah Gul University (AGU), Kayseri, Turkey. His current research interests are in next-generation wireless networks, wireless ad hoc and sensor networks, smart grid communications, and underwater networks